Front. Energy 2020, 14(4): 667–682
https://doi.org/10.1007/s11708-020-0695-y

REVIEW ARTICLE

Yanxing ZHAO, Maoqiong GONG, Haocheng WANG, Hao GUO, Xueqiang DONG

Development of mobile miniature natural gas liquefiers

Abstract With increasing consumption of natural gas (NG), small NG reservoirs, such as coalbed methane and oil field associated gas, have recently drawn significant attention. Owing to their special characteristics (e.g., scattered distribution and small output), small-scale NG liquefiers are highly required. Similarly, the mixed refrigerant cycle (MRC) is suitable for small-scale liquefaction systems due to its moderate complexity and power consumption. In consideration of the above, this paper reviews the development of mobile miniature NG liquefiers in Technical Institute of Physics and Chemistry (TIPC), China. To effectively liquefy the scattered NG and overcome the drawbacks of existing technologies, three main improvements, i.e., low-pressure MRC process driven by oil-lubricated screw compressor, compact cold box with the new designed heat exchangers, and standardized equipment manufacturing and integrated process technology have been made. The development pattern of "rapid cluster application and flexible liquefaction center" has been eventually proposed. The small-scale NG liquefier developed by TIPC has reached a minimum liquefaction power consumption of about 0.35 kW·h/Nm^3. It is suitable to exploit small remote gas reserves which can also be used in boil-off gas reliquefaction and distributed peak-shaving of pipe networks.

Keywords natural gas, mobile miniature liquefiers, mixed refrigerant cycle, vapor liquid equilibrium, heat transfer

Received Oct. 31, 2019; accepted May 15, 2020; online Sept. 15, 2020

Yanxing ZHAO, Haocheng WANG, Hao GUO
Key Laboratory of Cryogenics, Technical Institute of Physics and Chemistry, Chinese Academy of Sciences, Beijing 100190, China

Maoqiong GONG (✉), Xueqiang DONG
Key Laboratory of Cryogenics, Technical Institute of Physics and Chemistry, Chinese Academy of Sciences, Beijing 100190, China; University of Chinese Academy of Sciences, Beijing 100039, China
E-mail: gongmq@mail.ipc.ac.cn

1 Introduction

To control air pollution, optimize energy structure, and achieve sustainable development, China has promulgated serious policies [1–3]. As the cleanest fossil energy, natural gas (NG) proportion in the primary energy is expected to increase substantially in China. In July 2017, "Opinions on Accelerating the Use of Natural Gas" was proposed by the National Development and Reform Commission of the People's Republic of China [4], and cultivating NG as one of the main energy sources was emphasized.

NG proportion in the primary energy of China is gradually increasing, which was 7.8% in 2018, and will exceed 10% by 2020 and 15% by 2030, according to the government's work report [5]. However, it is still far below the average NG ratio of the world, which was more than 23.8% in 2018 [6,7]. In the near future, with the promotion of social development and welfare, a huge amount of NG will be demanded. However, NG production in China is insufficient, and thus the vast NG needed has to be imported. In other terms, China has become dependent on foreign NG in recent years. According to the National Bureau of Statistics, the proportion of imported NG rose to 42.9% in 2018, making China the largest importer of NG in the world [5].

China is relatively rich in NG resources. However, the distribution of these resources is very uneven. According to the National Bureau of Statistics, the gas reserves in China exceed 1×10^{14} Nm^3 [5]. However, more than 65% of these reserves is unconventional gas, i.e., coal bed methane, shale gas, and oil field associated gas. These gas fields are mostly small and medium-sized. The majority of them are located in remote areas (far away from the users), and the geological structure of most of the gas fields is relatively complex. Thus, from the technical and economical point of view, the traditional pipeline network and the centralized liquefaction transport mode are not suitable for these isolated and scattered fields. As a result, more than 3×10^{10} Nm^3 of coal bed methane are not utilized [8], which is enough to meet the NG demand in Beijing for about 1.5 a. This leads to a great waste of resources as well as

environmental contamination. Therefore, extraction of the unconventional NG is especially important in China for energy security and independence, besides environmental protection reasons. Under this background, there is an urgent need for the development of the mobile and flexible NG liquefaction technology.

In this paper, the current mainstream NG liquefaction technologies are reviewed, aiming to search for suitable technologies for isolated and scattered gas fields. Moreover, a mobile NG liquefier driven by oil-lubricated single-stage screw compressor designed by Technical Institute of Physics and Chemistry (TIPC) is introduced. Furthermore, the challenges as well as the development of this kind of mobile miniature NG liquefiers are presented.

2 Review of the current liquefaction technologies

In a liquefied natural gas (LNG) production plant, the NG is generally cooled from ambient temperature to approximately 120 K, and then stored in the liquefied form in a near-boiling state. Thus, NG liquefaction is a typical temperature-distributed heat load-cooling process. Figure 1 shows the temperature-enthalpy (T-h) diagram (at constant pressure varying from 1 to 10 MPa) for a specific NG [9] having the composition reported in Table 1. As the isobar of 5 MPa presented by the dashed line indicates, the liquefaction flow of NG can be divided into pre-cooling, condensation, and sub-cooling. According to the Second Law of Thermodynamics, as the temperature difference in heat transfer decreases, the entropy generation and the exergy loss decrease, too. Therefore, the decrement in temperature difference between NG and the coolant is crucial, especially in the low-temperature range. Based on this consideration, the liquefaction process is performed around the dew point line of NG, as shown in Fig. 1.

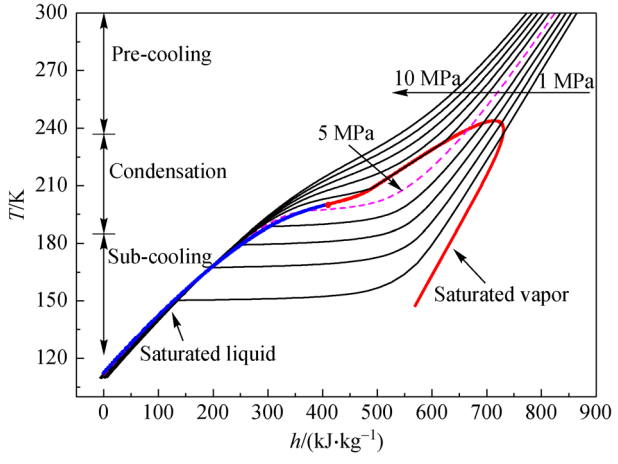

Fig. 1 Temperature-enthalpy (T-h) diagram (at constant pressure from 1 MPa to 10 MPa) as a function of temperature for a specific NG having the composition reported in Table 1.

To achieve the liquefaction of NG, both sensible and latent heat have to be removed over a wide temperature range (approximately 300 K to approximately 110 K). Therefore, to achieve the smallest temperature difference between NG and the coolant, one or more refrigerants (either single or cascaded) are employed. After years of development, the cascade refrigeration cycle (CRC), mixed refrigerant cycle (MRC), and reverse Brayton cycle (RBC) have become the main NG liquefaction technologies [10].

In the CRC system [11–13], generally, three pure refrigerant cycles (propane, ethylene, methane) each with a 3-stage compression are employed, as demonstrated in Fig. 2. The CRC achieves a high liquefaction efficiency due to the small temperature difference between NG and the coolant since there are 9-stage evaporation processes to match NG heat load. Meanwhile, the refrigerants in CRC are easily charged, owing to only one refrigerant for one cycle, which gives CRC good robustness. However, the system is complex and hard to maintain because it consists of nine compressors and nine heat exchangers.

In the RBC cycle [14–16] which is dominated by the N_2-based cycle (Fig. 3), a multi-stage expansion process is used. The cold box and equipment in RBC are simple. The liquefaction efficiency is relatively low but could be improved with the pre-cooling stage [17]. Besides, in some cases, NG can be used as the refrigerant medium, which requires no external refrigerant inventory and associated storage, thereby reducing the size and complexity of the liquefaction process [18,19].

In a single-stage MRC (SMRC) system [20,21] (Fig. 4), normally a single centrifugal compressor is used in a large-scale system. The mixed refrigerant consists of four to eight components to match NG heat load. The refrigerant concentration and the heat exchanger are crucial in achieving a high liquefaction efficiency. The suction pressure of the compressor varies from 0.1 to 0.3 MPa, while the discharge pressure varies from 3.5 to 5.0 MPa [21], which means the compression ratio will reach up to 20–30.

Table 1 Composition (on a molar basis) of a specific NG

Composition	Percent/%
Methane	94.59
Ethane	3.43
Propane	0.59
n-Butane	0.12
Iso-Butane	0.10
n-Pentane	0.03
Iso-Pentane	0.03
n-Hexane	0.05
Nitrogen	1.06

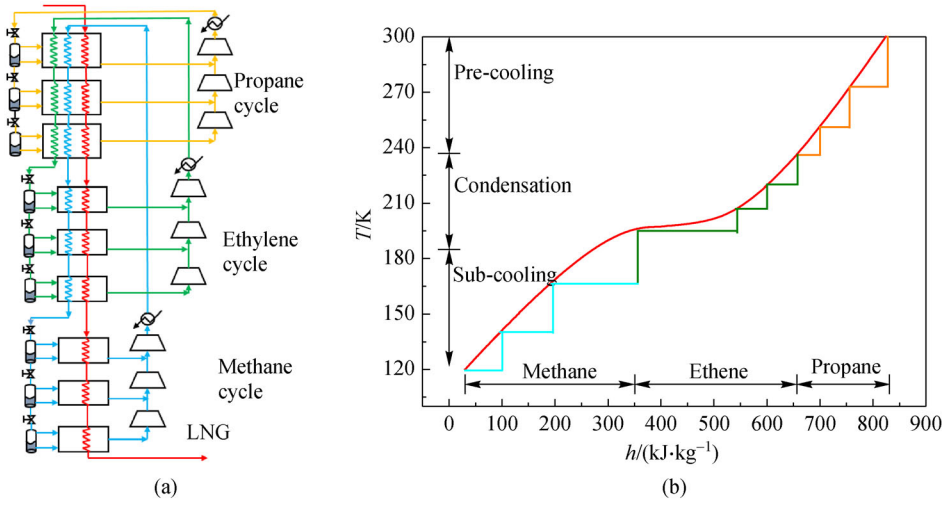

Fig. 2 Liquefaction cycle and temperature-enthalpy characteristic in RBC system.
(a) Schematic diagram of CRC system; (b) temperature-enthalpy (*T*-*h*) diagram for a specific NG having the composition reported in Table 1 at 5 MPa and refrigerants in CRC.

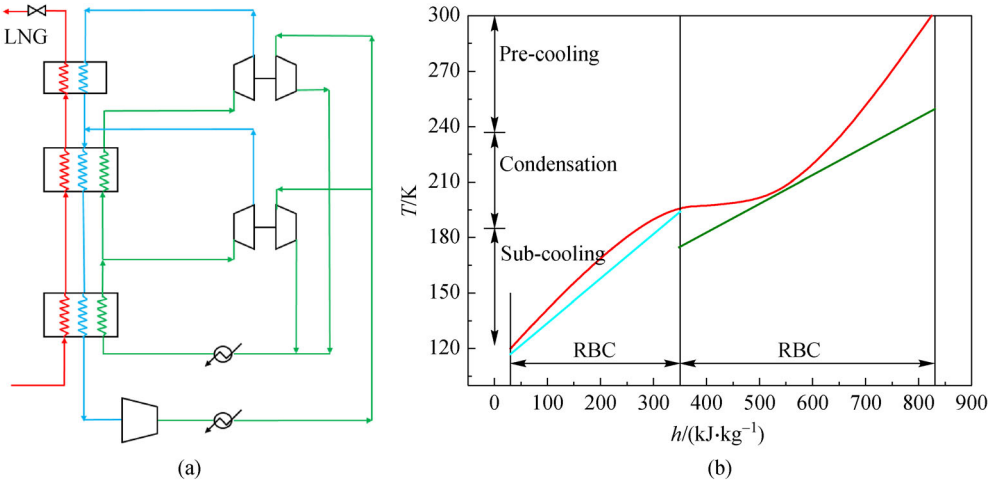

Fig. 3 Liquefaction cycle and temperature-enthalpy characteristic in RBC system.
(a) Schematic diagram of RBC system; (b) temperature-enthalpy (*T*-*h*) diagram for a specific NG having the composition reported in Table 1 at 5 MPa and refrigerants in RBC.

In both CRC and MRC, phase transition processes occur in the refrigerants, while the phase of the refrigerant does not change in expander-based technologies, which makes the configuration of RBC relatively simple. A notable disadvantage of RBC is the higher specific power requirement (compression power required for liquefying one unit of NG) compared to CRC and MRC [9,10,22–25]. CRC is still used in some large-scale factories (mainly constructed in the early days); however, it is not suitable in small-scale applications, especially for skid-mounted liquefaction systems due to its complexity and low efficiency. Therefore, most of the liquefaction systems for small-scale applications are developed based upon RBC and MRC or their modified cycles.

In the pre-cooling MRC system [26,27] (Fig. 5), the robustness of CRC and the high efficiency of SMRC can be integrated by a 3-stage propane cycle used for pre-cooling and an MRC cycle used for condensation and sub-cooling of NG. The liquefaction efficiency benefits from the heat load match in low-temperature areas. Since the MRC can be optimized and operated nearly independently of the pre-cooling propane cycle, the high boiling point refrigerant (e.g.,*iso*-butane and *iso*-pentane) is no longer needed. It was the most widely preferred cycle in the past decades. Recently, many works aiming at the selection of pre-cooling stage refrigerants have been reported [28–30].

As the name suggests, the dual-MRC (DMR) system [31,32] (Fig. 6) consists of two MRC systems: the pre-cooling MRC with high boiling points components, and the low-stage MRC with middle-low boiling point

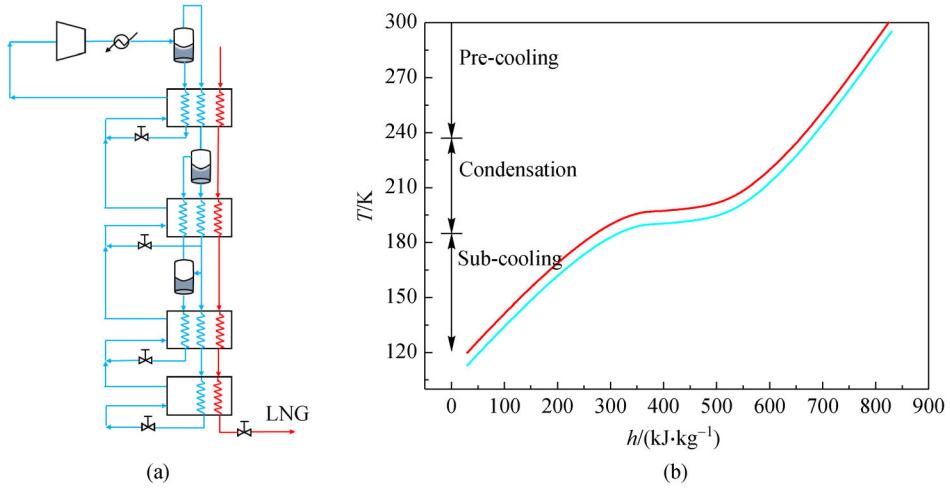

Fig. 4 Liquefaction cycle and temperature-enthalpy characteristic in MRC system.
(a) Schematic diagram of the MRC system; (b) temperature-enthalpy (*T*-*h*) diagram for a specific NG having the composition reported in Table 1 at 5 MPa and refrigerants in MRC.

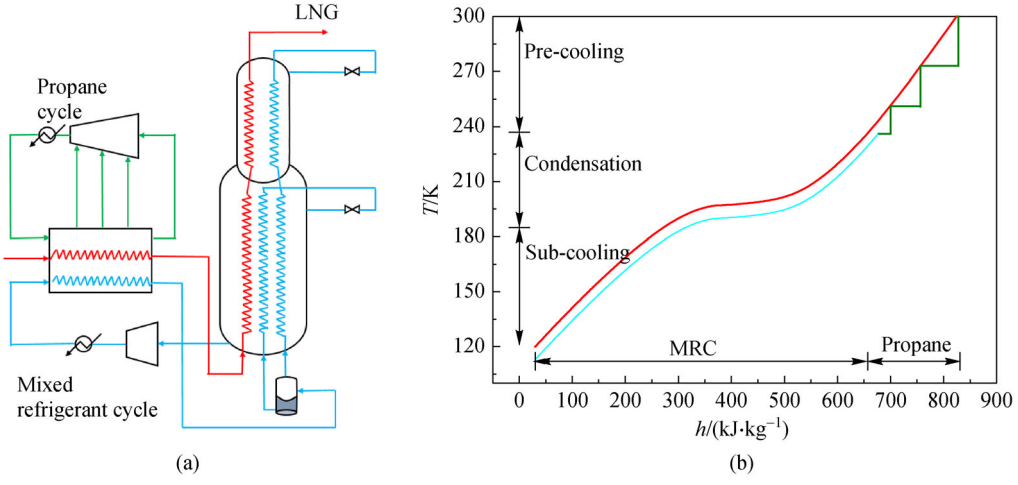

Fig. 5 Liquefaction cycle and temperature-enthalpy characteristic in C3-MRC system.
(a) Schematic diagram of C3-MRC system; (b) temperature-enthalpy (*T*-*h*) diagram for a specific NG having the composition reported in Table 1 at 5 MPa and refrigerants in C3-MRC.

components. One major reason why attention has been focused on DMR is that it can reduce propane inventory, compared to C3-MRC. High efficiency was achieved in DMR with a better match of heat load compared to SMR. In theory, it has the highest efficiency among the NG liquefaction cycles [33,34]. In real applications, the C3MR and DMR processes have similar efficiencies [35].

The cycle combining C3-MRC and N_2-RBC was proposed because it is difficult to achieve the uniform distribution of multi-component two-phase flow in the main heat exchanger in super large-scale applications [36]. This process is also called AP-X (Fig. 7) by the Air Products (AP) Company. The N_2-RBC loop in low stage benefits from the heat load match and the uniform distribution in the heat exchanger. With the aid of N_2-RBC at the low-temperature stage, this process may possess the largest liquefaction capacity with a reasonable production cost, although its thermodynamic efficiency is smaller than that of C3-MRC.

Although the power consumption of the liquefaction process is important for both small- and large-scale applications, each application has its own emphasis. The initial investment and compactness are of greater importance in small-scale LNG plants compared to large-scale ones.

Thus, some technologies with a low-power consumption of liquefaction efficiency are suitable for large-scale applications (e.g., the CRC process); however, they are not suitable for small-scale ones due to high capital cost and complexity. Besides, for onshore and offshore

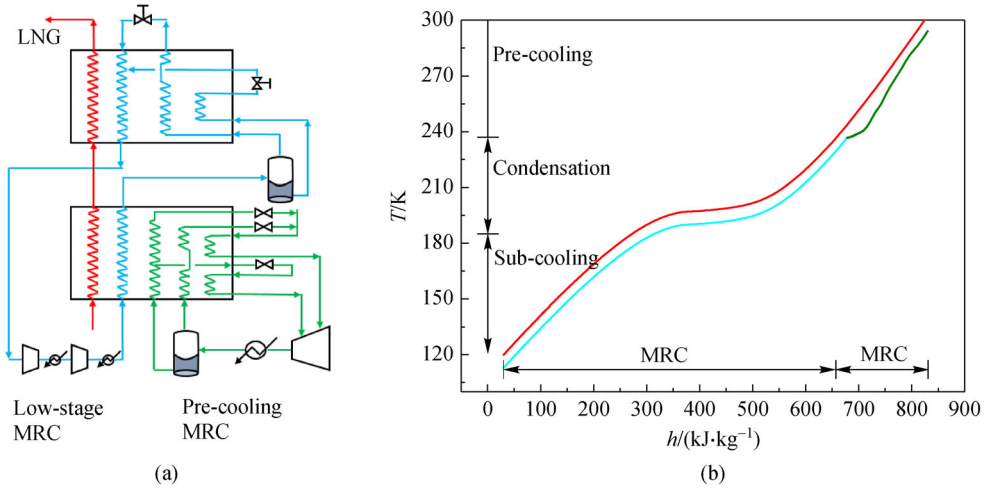

Fig. 6 Liquefaction cycle and temperature-enthalpy characteristic in dual-MRC system.
(a) Schematic diagram of dual-MRC system; (b) temperature-enthalpy (*T*-*h*) diagram for a specific NG having the composition reported in Table 1 at 5 MPa and refrigerants in dual-MRC.

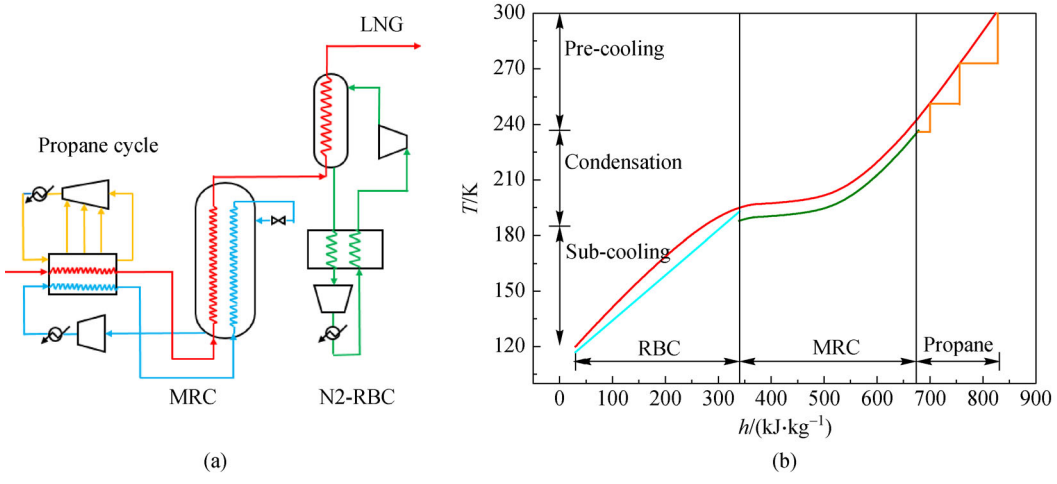

Fig. 7 Liquefaction cycle and temperature-enthalpy characteristic in C3-MR-N_2 system.
(a) Schematic diagram of C3-MR-N_2 system; (b) temperature-enthalpy (*T*-*h*) diagram for a specific NG having the composition reported in Table 1 at 5 MPa and refrigerants in C3-MR-N_2.

applications, different technologies are preferred. At present, MRC-based technologies still dominate the onshore LNG plant market, while RBC-based technologies are pursued in the offshore LNG market [37,38]. Table 2 presents a rough comparison of state-of-the-art NG liquefaction technologies. At present, for small scale, NG liquefaction applications, the precooling-MRC process, as well as the nitrogen-based RBC systems, receives the most attention. Although there is no clear agreement on the most suitable liquefaction process for small-scale applications, the precooling-MRC process, with relatively high efficiency, is quite promising to achieve high efficiency and

Table 2 Comparison of mainstream NG liquefaction technologies

Cycle	Efficiency	Complexity	Reliability	Possibility for miniaturization
CRC	High with 9 stages processes	High	Low	Too many facilities, low reliability
Precooling-MRC	High	Middle	High	Good, with off-the-shelf facilities, easy assembly
N_2-RBC	Low, improved by precooling	Low, simple system configuration	High	Difficult in miniature of turbine and compressor

reliability, once some problems, such as refrigerant composition control and the misdistribution of the two-phase flow, are resolved.

Considering the urgent NG need in China, and the fact that the conventional liquefaction technologies are not suitable for remote small-scale gas reservoirs, the use of low-pressure MRC driven by oil-lubricated single-stage screw compressor have been proposed in this paper, and accordingly high-efficiency, low-cost, and mobile NG liquefiers developed in Technical Institute of Physics and Chemistry (TIPC) in Chinese Academy of Sciences, China.

3 Development and applications of mobile miniature NG liquefiers

Several key problems aroused in developing the mobile miniature NG liquefier, such as the improvement of liquefaction, the decrease of the size of the key equipment (for example the cold box), and the shortening of the construction period of the liquefier and the lowering of the initial cost, which can be summarized as three challenges.

3.1 Challenge 1: liquefaction miniaturization

The conventional MRC system used for the NG liquefaction in large-scale LNG plants is very complex, which poses a challenging engineering problem to the miniaturization of the liquefaction system. The pressure of refrigerant in the cycle reaches up to 3–5 MPa [21], where the compression ratio increases to 20–30, yielding to the high requirements on the compressor. This is an oil-free multi-stage centrifugal compressor, monopolized by several companies, with high cost and is difficult to meet the miniaturization demand of the liquefaction system. These disadvantages make the construction period of a typical MRC system long and the relocation of it hard or even impossible. Besides, this kind of MRC system has poor adaptability and flexibility in dealing with varying duties.

3.1.1 Progress: low-pressure cycle using a screw compressor

To overcome the above-mentioned drawbacks of the high-pressure MRC process, a low-pressure cycle has been built. Compared to the high-pressure cycle employing an oil-free multi-stage centrifugal compressor, the low-pressure cycle can utilize an oil-lubricated screw compressor, which is widely used in HVAC&R (heating, ventilating and air conditioning and refrigerating). The benefits of oil-lubricated screw compressors are noticeable. First of all, approximate isothermal compression can be achieved by oil injection cooling in the screw compressor. Secondly, the semi-hermetic structure can avoid leakage of the mixed refrigerants, which frequently occurs in oil-free compressors. Finally, the off-the-shelf compressors are economic, highly reliable, and well-supplied, which can significantly reduce the initial manufacturing costs and shorten the manufacturing time.

3.1.2 Progress: low-pressure cycle with optimized mixtures

The selection of components for mixed refrigerants is a significant part of the thermal design of MRC. The optimal refrigerant in the low-pressure cycle is not the same as that in the high pressure cycle. At a suitable temperature of normal boiling point (T_{nb}) and a low triple-point temperature, N_2, CH_4, C_2H_4, C_2H_6, C_3H_8, and *iso*-C_4H_{10} have been widely used in recently developed MRC systems [35]. Therefore, two strategies have been proposed in this paper to give a better match for heat load and temperature in the new cycle.

First, tetrafluoromethane (R14), with a normal boiling temperature of 145.2 K, was introduced to the mixed refrigerant. It is a suitable bridge between methane and ethane, as shown in Fig. 8. Although R14 has a high global warming potential value, the use of R14 can improve the efficiency of the MRC system [39]. R14 can be replaced by ethene (R1150) for environmental protection, although the exergy efficiency of the MRC system will slightly decrease. Second, thermodynamic optimization of the mixed refrigerants based on isothermal throttling effect is applied. Isothermal throttling effect (Δh_T) corresponds to the cooling capacity gained after throttling. The throttling effects of several pure substances with different boiling points from N_2 to *iso*-C_5H_{12} are shown for various temperatures in Fig. 8. According to the analysis of Gong et al. [40], it is significant to get a component series with relaying temperature ranges of maximum throttle effect in the component selection for mixed refrigerants. A large mixture throttling effect could be achieved in the whole temperature region by relaying the maximum throttling effect of each component with each other. The minimum isothermal throttling effect of the mixture in the whole temperature region is larger than that of any pure component.

3.1.3 Progress: optimized mixtures with accurate properties

The cubic equations of state (EoS), such as Peng-Robinson (PR) [41], Redlich-Kwong (RK) [42], and Soave Redlich-Kwong (SRK) [43], are the most preferred models in liquefaction process simulation [44,45]. The cubic EoS cannot properly describe the liquid properties in most cases [41], especially for the mixtures. As a result, large discrepancies between computational results and experimental data may be introduced by these inaccuracies [46,47]. However, the prediction accuracy can be

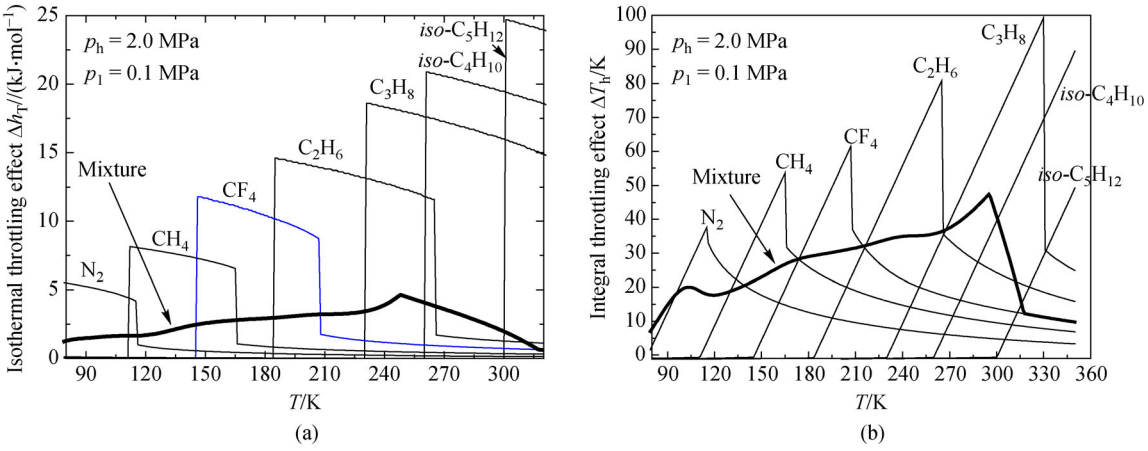

Fig. 8 Comparison of isothermal and integral throttling effects of mixture and pure components.
(a) Isothermal throttling effects of mixture and pure components; (b) integral throttling effects of mixture and pure components.

improved by experimental measurement of thermophysical properties, such as vapor-liquid equilibrium (VLE), vapor and liquid densities, and specific heat. Since for PR EoS, only one adjusting parameter (i.e., binary interaction parameter) is required to describe the thermophysical properties of the mixtures, which can be determined by regressing the experimental data [41,48–50]. As shown in Fig. 9, a series of apparatuses are established, including several VLE devices aimed at different temperature zones [48–50], one *pvT* measurement apparatus [51] based on Archimedes' principle of buoyancy, and one adiabatic batch calorimeter [52] for constant-volume specific heat. The accurate experimental data were used for the development of correlation and predictive thermodynamic models. For example, for the R14-based mixtures (R14 + R50, R14 + R170, R14 + R290), the estimated VLE (dashed line in Fig. 10) by setting binary interaction parameters $k_{ij} = 0$ by default presents a big deviation from the correlated VLE by experimental data, as shown in Fig. 10. This inaccuracy will definitely affect the simulation of the MRC system, and eventually lead to a large deviation between the design and actual construction. Therefore, the VLE, vapor and liquid densities, and isochoric specific heat data for more than 30 mixtures were measured, and the equation of state for simulation of MRC system was established [48–50]. This makes the

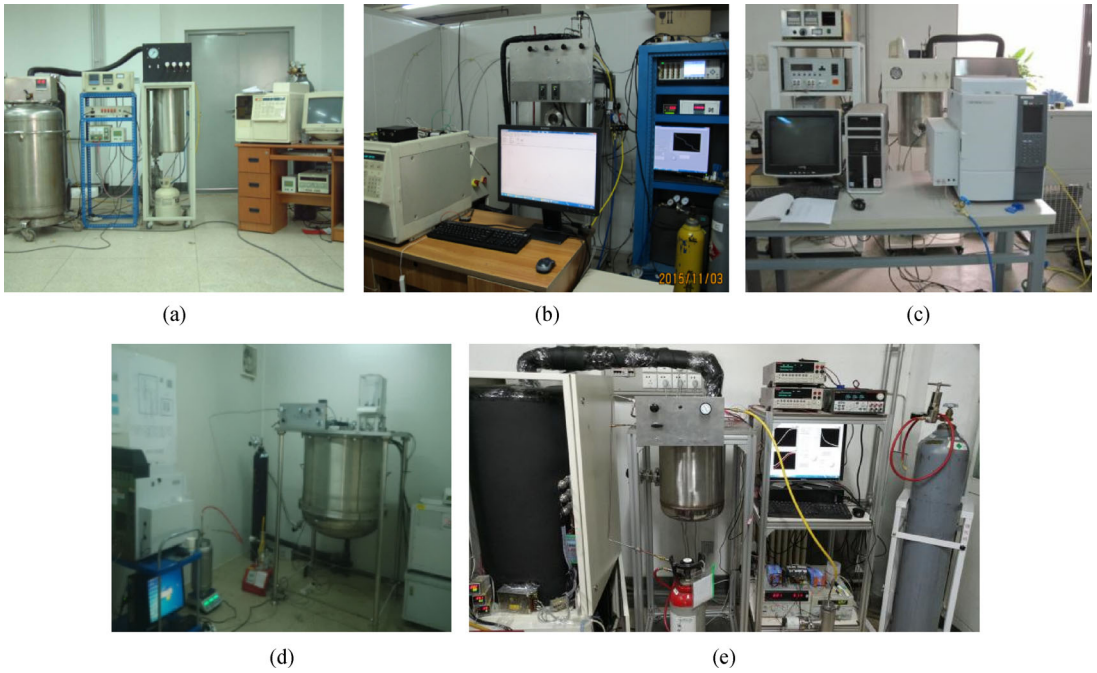

Fig. 9 Apparatuses built in the TIPC for thermophysical properties measurement.
(a) Low-temperature VLE apparatus; (b) middle-low-temperature VLE apparatus; (c) middle-high-temperature VLE apparatus; (d) density apparatus; (e) isochoric specific heat capacity apparatus.

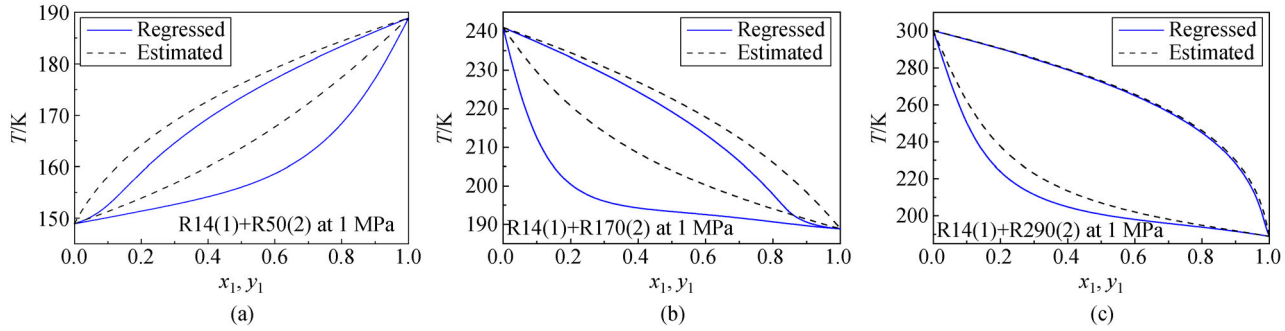

Fig. 10 Temperature-composition diagram for R14 + R50, R14 + R170, and R14 + R290 binary mixtures (The PR [41] equation is employed for regressing or estimating the VLE data. The solid lines are correlated by the experimental data ($k_{ij} \neq 0$), while the dashed line is predicted by setting the interaction parameter to 0 ($k_{ij} = 0$)).
(a) Vapor liquid equilibrium (VLE) data of R14 + R50 mixture; (b) VLE data of R14 + R170 mixture; (c) VLE data of R14 + R290 mixture.

simulations more convincing, compared to other simulations/works supported with no experimental data. At last, the mixture consisting of N_2, CH_4, CF_4 (or C_2H_4), C_2H_4, C_2H_6, C_3H_8, and iC_4H_{10} is selected for the MRC system.

3.1.4 Progress: low-pressure cycle with a dephlegmator

Although the energy efficiency of the refrigeration cycle (Cycle A without separation) is the highest, as shown in Figs. 11 and 12, the lubricant and high-boiling components may freeze at the low-temperature part of the heat exchangers and block the flow channels. Therefore, a single-stage dephlegmation cycle (Cycle E) was developed by Wu et al.[53] and Gong et al. [54], as shown in Fig. 12(b).

A dephlegmator, shown in Fig. 13 [49], is used for replacing the flash phase separator in the traditional MRC. In the dephlegmator, the lubricant and high-boiling components are separated by the dephlegmation effect with the cooling power supplied by the backflow low-pressure mixed refrigerant. Since the backflow provides a low condensation trapping surface temperature, the dephlegmator has a better separation performance than the flash separator. The detailed thermodynamic simulation of the dephlegmator was conducted by Li et al. [55]. The high-boiling components in the liquid phase had a high recovery ratio of more than 90%, and the energy consumption was decreased by more than 30% compared to the traditional distillation tower with similar separation effects. In conclusion, when the efficiency of the optimized separation cycle is close to (or just slightly lower than) the cycle without separation, the separation cycle with the dephlegmator achieves a high efficiency and reliability [56].

3.1.5 Progress: practical effect of low-pressure liquefaction process

Finally, the low-pressure liquefaction system was built. The highest pressure of the mixed refrigerant reached up to 1.5–2.0 MPa, with a pressure ratio varying from 3 to 5. Compared to the high-pressure MRC system [21], at the highest pressure of 3.0–5.0 MPa and the pressure ratio of 20 to 30, the low-pressure MRC significantly eased the design and manufacturing of the critical components, such as compressor and heat exchanger. The intrinsic exergy efficiency of the MRC system with new mixed refrigerants (R14) reaches up to 60%, i.e., increased by 70% (Fig. 14) compared to the conventional high-pressure MRC system (with an intrinsic exergy efficiency of 35%).

The intrinsic exergy efficiency is defined as the maximum exergy efficiency of a MRC system by optimizing the molar concentration of the given components at a given high pressure p_h, low pressure p_l, ambient temperature T_0, and refrigeration temperature T_c. The compressing process is assumed to be an adiabatic process without entropy increase and the pressure drop of the mixed refrigerants is zero. In other words, the highly idealized cycle has no extrinsic losses but only intrinsic losses. Therefore, the thermodynamic performance of the ideal cycle only depends on the mixed refrigerant used, the operating pressures, and the cycle configuration. The exergy efficiency is calculated as the ratio of exergy gained by liquefied gas to the inputted exergy. The exergy gained liquefied gas is the exergy difference between inlet and outlet status. The detailed exergy model can be seen in Ref. [40].

$$\eta = \frac{\text{Exergy}_{\text{gained}}}{\text{Exergy}_{\text{input}}} = \frac{E_{Q_c}}{W} = 1 - \frac{\sum \Pi_j}{W}, \tag{1}$$

where η is the intrinsic exergy efficiency of the cycle; E_{Q_c} is the exergy of the temperature-distributed heat loads, in which Q_c is the heat loads; W is the electrical power consumed, and Π_j is the exergy loss of each element j in the cycle. The intrinsic losses depend on the thermodynamic processes of the cycle and mixed refrigerant properties, such as the throttle irreversibility, the heat transfer

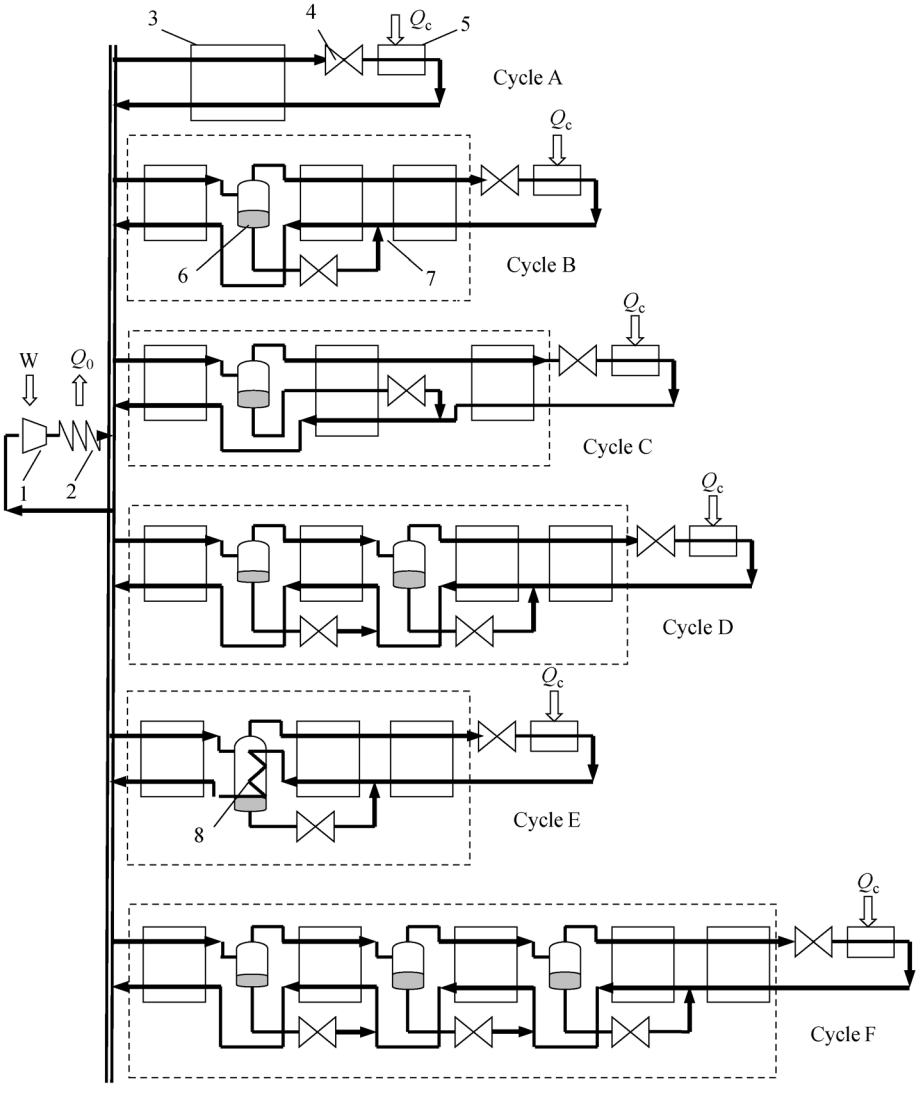

1—compressor; 2—aircooler; 3—heat exchanger; 4—throttle valve; 5—evaporator; 6—gas liquid separator; 7—mixer; 8—dephlegmator; Q_c—heat loads; Cycle A—no separation; Cycle B—single-stage separation; Cycle C—modified single-stage separation; Cycle D—two-stage separation; Cycle E—single-stage separation with a dephlegmator; Cycle F—three-stage separation

Fig. 11 Several mixed refrigerant cycles driven by single-stage compressor.

temperature difference between the cold and hot streams in the heat exchangers.

3.2 Challenge 2: heat transfer and cold box

The low-pressure cycle makes it possible to liquefy the NG driven by the oil-lubricated screw compressor. However, this inevitably reduces the volumetric refrigeration capacity (i.e., kg LNG per volume flow rate of refrigerant). As a result, the heat load of the main heat exchanger for NG liquefaction is almost tripled, which negatively affects the volume of heat exchangers. Furthermore, due to the lack of complex two-phase heat transfer for the multi-component mixtures, it is always challenging to achieve the good two-phase flow mass-distribution in heat exchangers. Conventionally, excessive redundant design for the heat exchanger is adopted, leading to an oversized cold box, which further limits mobility.

3.2.1 Progress: basic heat transfer research

Three visualization testbeds (for nucleate pool boiling [59], flow boiling [60] and flow condensation [61] heat transfer measurement) were set in TIPC (Fig. 15) to investigate the basic heat transfer characteristics. In Refs. [53–59], experiments were performed on nucleate pool boiling,

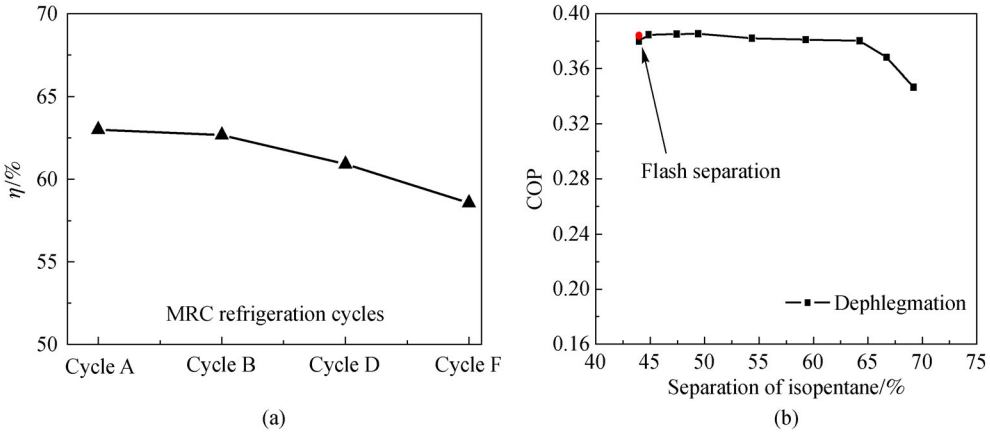

Fig. 12 Performance comparison of MRCs.
(a) With various stages of phase separators; (b) cycle E with a dephlegmator.

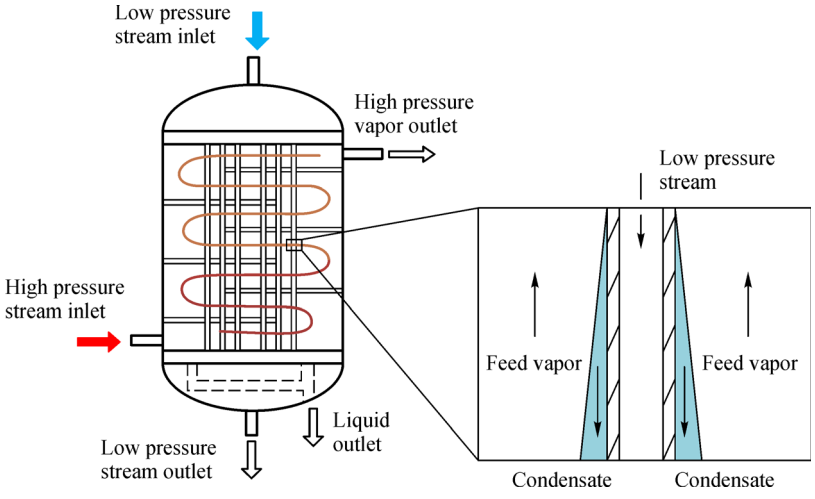

Fig. 13 Detailed structure of dephlegmator in TIPC.

flow boiling, and flow condensation heat transfer of some refrigerants and their mixtures, and new correlations were proposed for two-phase heat transfer and fluid flow with a good accuracy [59–67].

3.2.2 Progress: heat exchangers

A new heat exchanger configuration (Fig. 16) was proposed [68], where the invented plate-fin exchangers with varying cross-sections achieved the two-phase flow velocity regulation and the even-distribution of two-phase flow [69–73]. Simulations and experimental tests were performed to further optimize the structure of the new exchangers [74].

3.2.3 Progress: compact cold box

Based on the research on the heat transfer of mixed refrigerants and the recently designed heat exchangers, a compact cold box, a combined plate-fin, and spiral wound heat exchangers were designed and manufactured, which resulted in a high efficiency and a low flow resistance. As a result, the compact cold box was shortened from 10 to 15 m to 3 m. As expected, it has quite a good mobility, allowing the compact box to be mounted on a truck. Figure 17 shows the compact liquefier equipped with a compressor and a cold box.

3.3 Challenge 3: fast construction technology

The traditional stationary LNG factories were not designed in the skid-mounted process module; thus, they require a long construction period (normally 8 to 18 months). All facilities are fixed, i.e., they have a poor mobility. Moreover, the long test (debugging) period is ineluctable. Therefore, they are not very useful for scattered gas resources/fields.

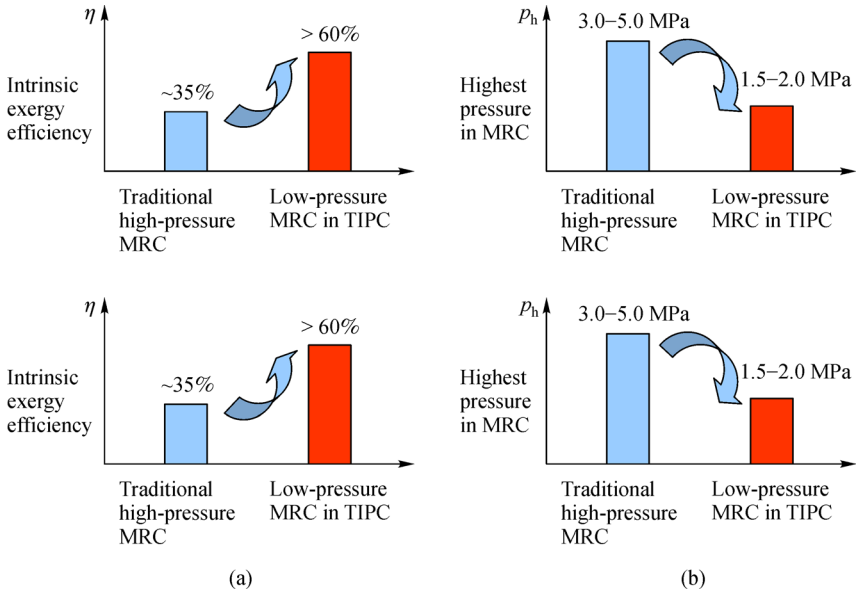

Fig. 14 Intrinsic exergy efficiency and highest refrigerant pressure of low-pressure MRC compared to those of high-pressure MRC (Data from Ref.[58]).

(a) Comparison of intrinsic exergy efficiency; (b) comparison of highest refrigerant pressure.

Fig. 15 Apparatuses built in TIPC for the measurement of heat transfer properties.

(a) Nucleate pool boiling apparatus; (b) flow boiling apparatus; (c) flow condensation apparatus.

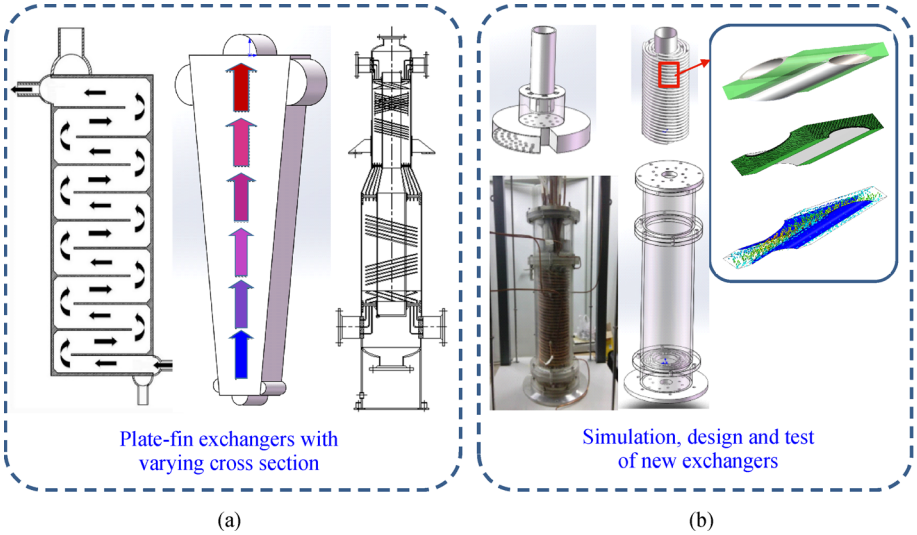

Fig. 16 Plate-fin exchangers and spiral wounded heat exchangers designed by TIPC.

(a) Heat exchangers with varying cross section; (b) simulation, design and test of the heat exchangers.

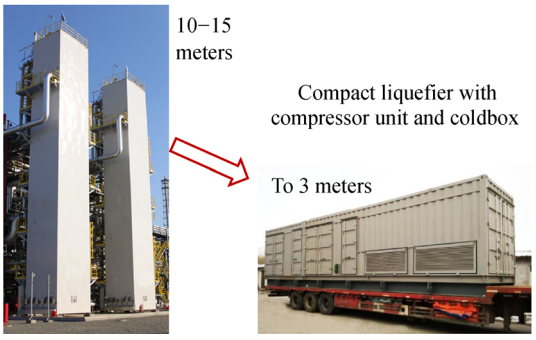

Fig. 17 Compact cold box designed by TIPC.

3.3.1 Progress: customized normalization technology

Standardized equipment manufacturing and integrated process technology (Fig. 18) have been available after years of effort. Three main technologies, namely production and testing, mixed refrigerants charging, and fast construction have been normalized. Specifically, the liquefaction plant is composed of/divided into several modules (compressor and oil separator module, cold box module and air cooler and fan module), and each module is manufactured on a skid. Combining with modularization interface design, the equipment can be easily and quickly assembled on a trailer skid. Besides, a series of processes and equipment are designed for mixed refrigerants charging.

3.3.2 Progress: flexible liquefaction center

High quality and low-cost are achieved by the standardized equipment manufacturing and device debugging technologies. The construction period is shortened from 8 months (for the traditional construction model) to only 2–6 weeks. In simple terms, “plug and liquefy” has been achieved. In addition, the development patterns of “rapid cluster application and flexible liquefaction center” has been eventually proposed. The flexible liquefaction center (Fig. 19) requires a much lower initial investment/cost than the traditional fixed plants. The reason for this is that the model proposed by the authors of the present paper can be built step by step. The profit of running liquefiers can support the installation of additional liquefiers. Another benefit is the flexibility in dealing with the unsteady gas resources. For example, the skid-mounted liquefier can be easily changed into a new gas well when the original one is exhausted.

3.3.3 Progress: performance comparison

The liquefier was built based on the aforementioned low-pressure MRC process, with an NG engine driving the screw compressor. All the liquefier components were integrated into a skid. The experimental results show that the NG engine consumes about 11% of the feed gas to liquefy the remaining 89% [29]. By using the off-the-shelf equipment and normalization technologies, the initial cost

(a) (b)

Fig. 18 Standardized equipment manufacturing and integrated process technology.
(a) Normalization of facility production, compressor module; (b) modularization in construction of LNG factory.

Fig. 19 Flexible liquefaction center.

has been notably reduced. Now, it is about USD 2 million for a 10000 Nm^3/d liquefier and will be even lower for large-scale plants, which is comparative to large-scale liquefier.

Table 3 compares the performance of representative LNG devices. As reviewed by Song et al. [75], hundreds of simulations have been performed, but only few reported the experimental results of the NG liquefaction processes. Thus, most of the data presented in Table 3 are estimated from the website of the companies. The liquefaction devices of the TIPC are notably enhanceed compared to the ones of the same scale. Currently, more than 20 sets of LNG plants based on technology proposed by the authors of the present paper have been applied in Inner Mongolia Autonomous Region, Shanxi, Shaanxi, and Yunnan provinces, just to name a few. The development process of the LNG plants of TIPC can be seen from Fig. 20. At present, all liquefiers are skid-mounted with a good mobility.

4 Conclusions

This paper reviewed the development of mobile miniature NG liquefiers in TIPC. To efficiently liquefy the scattered NG and overcome the drawbacks of existing technologies, three main improvements have been made.

First, a low-pressure MRC process was built, including three key components: a low-pressure cycle for NG liquefaction, a mixed refrigerant with good intrinsic efficiency, and a cycle driven by an oil-lubricated screw compressor. The use of off-the-shelf components in constructing the liquefaction facility has greatly shortened the manufacturing time and reduced the costs related.

Next, a compact cold box with high efficiency was designed, including two main improvements: new heat exchangers and a compact cold box with a height below 3 m.

Lastly, the standardized equipment manufacturing and the integration processes were relized, including three main normalized technologies: mixed refrigerants charging normalization, production, test normalization, and fast construction normalization. The development patterns of "rapid cluster application and flexible liquefaction center" were eventually proposed.

The current small-scale NG liquefier achieved a minimum liquefaction power consumption of about 0.35 $kW \cdot h/Nm^3$. This made it suitable for small remote gas

Table 3 Comparison of the representative small-scale LNG devices

No.	Companies or institutes	Liquefaction technology	Scale/(10^4 $Nm^3 \cdot d^{-1}$)	Power consumption /($kW \cdot h \cdot N^{-1}m^{-3}$)	Percentage of consumed gas[a]
1	GTI (U.S.) [76]	MRC	0.2	0.947	29.6
2	Wärtsilä (Norway)[1]	MRC	6.7	0.50	15.6
3	SINTEF (Norway) [77]	MRC	2	0.6	18.8
4	Hamworthy (UK)[2]	N_2-RBC	10	0.57	17.8
5	Galileo (Argentina)[3]	N/A	2	0.65	20.3
6	KL energy [78]	MRC	100	0.48	15.0
7	ZY green energy [79]	CRC	92	0.48	15.0
8	ZJU [25, 80]	MRC	0.0025	0.5	15.6
9	HEB SL[4]	MRC	7	0.47	14.7
10	KR petroleum[5]	MRC	5	1.87	58.4
11	Yinchuan Tianjia[6]	N_2-RBC	10	0.65	20.3
12	Tianjin Zhenjin[7]	MRC	5	0.37	11.6
13	Sichuan KF[8]	MRC	100	0.39	12.2
14	SSCS[9]	Dual-MRC	250	0.9	28.1
15	Xinxing New Energy[10]	MRC	100	0.40	12.5
16	Liu [81]	N_2-RBC	15	0.47	14.7
17	TIPC	MRC	3	0.35	10.9

Notes: a— Percentage of the feed gas consumed to liquefy the remaining NG. Here, the efficiency of the natural-gas generator is estimated as 3.2 $kW \cdot h/Nm^3$. 1. Biogas liquefaction plant supplied by Wärtsilä to produce biofuel for buses in Norway. 2014–02–12, available at the website of wartsila.com; 2. Small scale & mini LNG liquefaction system. 2020–6–13, available at the website of hamworthy.com; 3. With Cryobox, Galileo achieves mid-scale LNG production. 2020–06–13, avaiable at the website of Galileo Technologies Company; 4. A 70000 Nm^3/d LNG liquefaction device. 2015–10–15, available at the website of Liaoning CIMC Hashenleng gas; 5. Small-scale LNG Equipment. 2015–04–01, available at the website of Shandong Kerui Petroleum Equipment CO., LTD; 6. Mobile natural gas liquefaction plant. 2016–04–09, available at website of Yinchuan Tianjia Energy Technology Co., Ltd; 7. 50000 Nm^3/d skid-mounted natural gas plant in Inner Mongolia. 2015–05–08, available at the website of Tianjin Zhenjin Oil and Gas Co., Ltd; 8. One million scale of natural gas liquefaction plant in Zhangjiakou. 2014–05–27, available at the website of Sichuan Air Separation Equipment; 9. China Huanqiu Contracting & Engineering Corp. The1st China LNG Expo. 2015; 10. LNG introduction. 2009–1–17, available at the website of Xingxing Energy

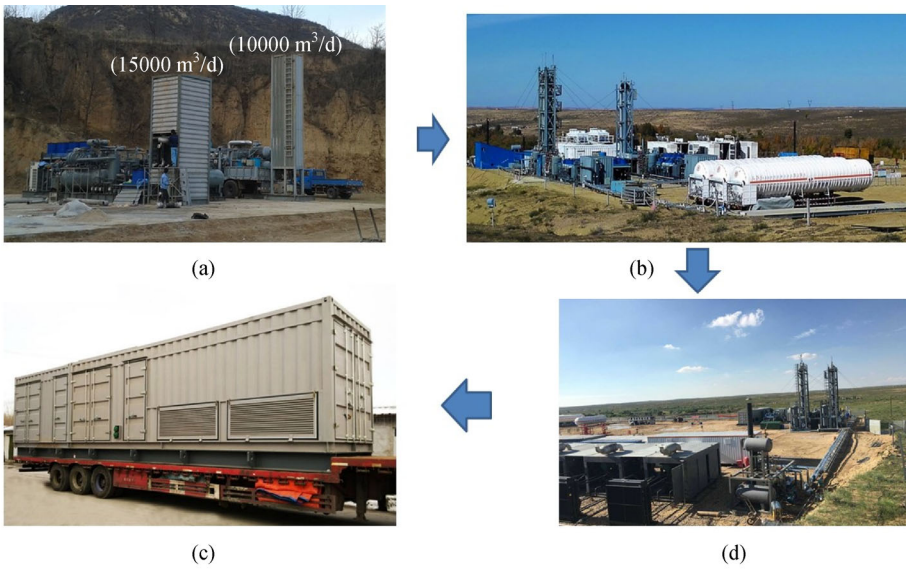

Fig. 20 Development process of LNG plants of TIPC: all equipment skid-mounted with good mobility. (a) Manufactured in 2012; (b) manufactured in 2014; (c) manufactured in 2015; (d) manufactured in 2016.

reserves, which could also be used in boil-off gas reliquefaction and the distributed peak-shaving of pipe networks.

Acknowledgements This work was financially supported by the National Natural Sciences Foundation of China (Grant Nos. 51625603 and 51876215), and the International Partnership Program of the Chinese Academy of Sciences (Grant No. GJHZ1876).

References

1. Shi G, Jing Y, Wang S, Zhang X T. Development status of liquefied natural gas industry in China. Energy Policy, 2010, 38(11): 7457–7465
2. Zhang G, Dou L, Xu Y. Opportunities and challenges of natural gas development and utilization in China. Clean Technologies and Environmental Policy, 2019, 21(6): 1193–1211
3. Zou C, Zhao Q, Chen J, Li J, Yang Z, Sun Q, Lu J, Zhang G. Natural gas in China: development trend and strategic forecast. Natural Gas Industry B, 2018, 5(4): 380–390
4. National Development and Reform Commission of the People's Republic of China. Opinions on accelerating the utilization of natural gas. 2017–7–4, available at website of ndrc.gov.cn
5. National Bureau of Statistics of the People's Republic of China. The national economic and social development statistical bulletin in 2016. 2017–2–28, available at the website of stats.gov.cn
6. National Bureau of Statistics. China Statistical Yearbook. 2018–5–29, available at the website of stats.gov.cn
7. BP. BP statistical review of world energy. 2019–07–30, available at the website of BP company
8. Miller S, Michalak A, Detmers R, Hasekamp O P, Bruhwiler L M P, Schwietzke S. China's coal mine methane regulations have not curbed growing emissions. Nature Communications, 2019, 10(1): 303
9. He T, Liu Z, Ju Y, Parvez A M. A comprehensive optimization and comparison of modified single mixed refrigerant and parallel nitrogen expansion liquefaction process for small-scale mobile LNG plant. Energy, 2019, 167: 1–12
10. Qyyum M, Qadeer K, Lee M. Comprehensive review of the design optimization of natural gas liquefaction processes: current status and perspectives. Industrial & Engineering Chemistry Research, 2018, 57(17): 5819–5844
11. Kanoğlu M. Exergy analysis of multistage cascade refrigeration cycle used for natural gas liquefaction. International Journal of Energy Research, 2002, 26(8): 763–774
12. Lee I, Tak K, Kwon H, Kim J, Ko D, Moon I. Design and optimization of a pure refrigerant cycle for natural gas liquefaction with subcooling. Industrial & Engineering Chemistry Research, 2014, 53(25): 10397–10403
13. Andress D, Watkins R. Beauty of simplicity: Phillips optimized cascade LNG liquefaction process. AIP Conference Proceedings, 2004, 710: 91–100
14. He T, Ju Y. Performance improvement of nitrogen expansion liquefaction process for small-scale LNG plant. Cryogenics, 2014, 61: 111–119
15. He T, Ju Y. A novel conceptual design of parallel nitrogen expansion liquefaction process for small-scale LNG (liquefied natural gas) plant in skid-mount packages. Energy, 2014, 75: 349–359
16. Chang H, Chung M, Lee S, Choe K H. An efficient multi-stage Brayton-JT cycle for liquefaction of natural gas. Cryogenics, 2011, 51(6): 278–286
17. Yuan Z, Cui M, Xie Y, Li C. Design and analysis of a small-scale natural gas liquefaction process adopting single nitrogen expansion with carbon dioxide pre-cooling. Applied Thermal Engineering,

2014, 64(1–2): 139–146
18. Chen S, Niu L, Zeng Q, Li X, Lou F, Chen L, Hou Y. Thermodynamic analysis on of skid-mounted coal-bed methane liquefaction device using cryogenic turbo-expander. IOP Conference Series, Materials Science and Engineering, 2017, 278(1): 012027
19. Ancona M, Bianchi M, Branchini L, De Pascale A, Melino F. Performance increase of a small-scale liquefied natural gas production process by means of turbo-expander. Energy Procedia, 2017, 105: 4859–4865
20. Swenson L K. Single mixed refrigerant, closed loop process for liquefying natural gas. US Patent, 05/739793, 1977
21. Nogal F, Kim J, Perry S, Smith R. Optimal design of mixed refrigerant cycles. Industrial & Engineering Chemistry Research, 2008, 47(22): 8724–8740
22. Chang H. A thermodynamic review of cryogenic refrigeration cycles for liquefaction of natural gas. Cryogenics, 2015, 72: 127–147
23. Remeljej C, Hoadley A. An exergy analysis of small-scale liquefied natural gas (LNG) liquefaction processes. Energy, 2006, 31(12): 2005–2019
24. Nguyen T, Rothuizen E, Markussen W, Elmegaard B. Thermodynamic comparison of three small-scale gas liquefaction systems. Applied Thermal Engineering, 2018, 128: 712–724
25. Wang Q, Song Q, Zhang J, Liu R, Zhang S, Chen G. Experimental studies on a natural gas liquefaction process operating with mixed refrigerants and a rectifying column. Cryogenics, 2019, 99: 7–17
26. Pillarella M, Liu Y N, Petrowski J, Bower R. The C3MR liquefaction cycle: versatility for a fast growing, ever changing LNG industry. In: Gas Technology Institute–15th International Conference and Exhibition on Liquified Natural Gas 2007, Barcelona, Spain, 2007, 1: 139–152
27. Gaumer L, Newton C. Combined cascade and multicomponent refrigeration system and method. US Patent, 05/002447, 1973
28. Castillo L, Majzoub Dahouk M, Di Scipio S, Dorao C A. Conceptual analysis of the precooling stage for LNG processes. Energy Conversion and Management, 2013, 66: 41–47
29. Gong M, Wu J, Sun Z, Liu J, Hu Q. Development and performance test of a small trailer-mounted moveable natural gas liquefier. Energy Conversion and Management, 2012, 57: 148–153
30. Castillo L, Dorao C. On the conceptual design of pre-cooling stage of LNG plants using propane or an ethane/propane mixture. Energy Conversion and Management, 2013, 65: 140–146
31. Newton C. Dual mixed refrigerant natural gas liquefaction with staged compression. US Patent, 4525185, 1985
32. Gadhiraju V, Timmerhaus Klaus D. Rizzuto C. Cryogenic Mixed Refrigerant Processes. New York: Springer, 2008
33. Khan M S, Karimi I, Lee M. Evolution and optimization of the dual mixed refrigerant process of natural gas liquefaction. Applied Thermal Engineering, 2016, 96: 320–329
34. Hwang J, Roh M, Lee K. Determination of the optimal operating conditions of the dual mixed refrigerant cycle for the LNG FPSO topside liquefaction process. Computers & Chemical Engineering, 2013, 49: 25–36
35. Bukowski J D, Liu Y N, Pillarella M R, Boccella S J, Kennington W A. Natural gas liquefaction technology for floating LNG facilities. In: 17th International Conference & Exhibition on Liquefied Natural Gas 2013 (LNG 2013), Houston, TX, USA, 2013, 2: 1342–1353
36. Chang H, Park J, Gwak K, Choe K H. Nitrogen expander cycles for large capacity liquefaction of natural gas. AIP Conference Proceedings, 2014, 1573: 1652–1657
37. Khan M, Karimi I, Wood D. Retrospective and future perspective of natural gas liquefaction and optimization technologies contributing to efficient LNG supply: a review. Journal of Natural Gas Science and Engineering, 2017, 45: 165–188
38. He T, Karimi I, Ju Y. Review on the design and optimization of natural gas liquefaction processes for onshore and offshore applications. Chemical Engineering Research & Design, 2018, 132: 89–114
39. Maytal B, Pfotenhauer J. Mixed coolant cryocooling. In: Miniature Joule-Thomson Cryocooling. New York: Springer, 2013, 277–334
40. Gong M, Wu J, Luo E. Performances of the mixed-gases Joule–Thomson refrigeration cycles for cooling fixed-temperature heat loads. Cryogenics, 2004, 44(12): 847–857
41. Peng D, Robinson D. A new two-constant equation of state. Industrial & Engineering Chemistry Fundamentals, 1976, 15(1): 59–64
42. Redlich O, Kwong J. On the thermodynamics of solutions. V. An equation of state. Fugacities of gaseous solutions. Chemical Reviews, 1949, 44(1): 233–244
43. Soave G. Equilibrium constants from a modified Redlich-Kwong equation of state. Chemical Engineering Science, 1972, 27(6): 1197–1203
44. Nguyen T, Elmegaard B. Assessment of thermodynamic models for the design, analysis and optimisation of gas liquefaction systems. Applied Energy, 2016, 183: 43–60
45. Austbø B. Use of optimization in evaluation and design of liquefaction processes for natural gas. Dissertation for the Doctoral Degree. Trondheim: Norwegian University of Science and Technology, 2015
46. Dauber F, Span R. Modelling liquefied-natural-gas processes using highly accurate property models. Applied Energy, 2012, 97: 822–827
47. Yuan Z, Cui M, Song R, Xie Y. Evaluation of prediction models for the physical parameters in natural gas liquefaction processes. Journal of Natural Gas Science and Engineering, 2015, 27: 876–886
48. Zhao Y, Dong X, Gong M, Guo H, Shen J, Wu J. Apparatus for low-temperature investigations: phase equilibrium measurements for systems containing ammonia. Journal of Chemical & Engineering Data, 2016, 61(11): 3883–3889
49. Dong X, Gong M, Shen J, Wu J. Vapor-liquid equilibria of the trans-1, 3, 3, 3-tetrafluoropropene (R1234ze (E))+ *iso*butane (R600a) system at various temperatures from (258.150 to 288.150) K. Journal of Chemical & Engineering Data, 2012, 57(2): 541–544
50. Guo H, Gong M, Dong X, Wu J. A static analytical apparatus for vapour pressures and (vapour + liquid) phase equilibrium measurements with an internal stirrer and view windows. Journal of Chemical Thermodynamics, 2014, 76: 116–123
51. Gong M, Li H, Guo H, Dong X, Wu J F. Apparatus for accurate density measurements of fluids based on a magnetic suspension balance. AIP Conference Proceedings, 2012, 1434(57): 1857–1864
52. Zhong Q, Dong X, Zhao Y, Wang J, Zhang H, Li H, Guo H, Shen J,

Gong M. Adiabatic calorimeter for isochoric specific heat capacity measurements and experimental data of compressed liquid R1234yf. Journal of Chemical Thermodynamics, 2018, 125: 86–92

53. Wu J F, Gong M Q, Liu J L, Luo E C, Qi Y F, Hu Q C. A new type mixture refrigeration auto-cascade cycle with partial condensation and separation reflux exchanger and its preliminary experimental test. Advances in Cryogenic Engineering, 2002, 613(1): 887–892
54. Gong M Q, Wu J F, Luo E C, Qi Y F, Hu Q C, Zhou Y. Further development of the mixture refrigeration cycle with a dephlegmation separator. In: Ross R G, eds. Cryocoolers. Boston: Springer, 2003: 603–608
55. Li M, Gong M, Guo H, Sun Z, Wu J. Steady-state thermodynamic simulation and structural design of the dephlegmator used in mixed-refrigerant Joule-Thomson refrigerators. Applied Thermal Engineering, 2016, 106: 480–492
56. Wu J, Gong M, Luo E. A mixed refrigerants Joule-Throttling cryogenic refrigeration cycle system with a dephlegmator. China Patent, ZL 00136709.9, 200 (in Chinese)
57. Wu J, Gong M, Dong X, et al.A gas cryogenic liquefaction separation system using separation effect of dephlegmator. China Patent, ZL200910090844.9, 2011 (in Chinese)
58. Gong M, Wu J, Luo E. Principle and Application of Mixed-Refrigerant Joule Thompson Refrigeration Technology. Beijing: China Science and Technology Press, 2014 (in Chinese)
59. Sun Z, Gong M, Li Z, Wu J. Nucleate pool boiling heat transfer coefficients of pure HFC134a, HC290, HC600a and their binary and ternary mixtures. International Journal of Heat and Mass Transfer, 2007, 50(1–2): 94–104
60. Zou X, Gong M, Chen G, Sun Z H, Zhang Y, Wu J F. Experimental study on saturated flow boiling heat transfer of R170/R290 mixtures in a horizontal tube. International Journal of Refrigeration, 2010, 33 (2): 371–380
61. Zhuang X, Gong M, Zou X, Chen G F, Wu J F. Experimental investigation on flow condensation heat transfer and pressure drop of R170 in a horizontal tube. International Journal of Refrigeration, 2016, 66: 105–120
62. Chen H, Chen G, Zou X, Yao Y, Gong M. Experimental investigations on bubble departure diameter and frequency of methane saturated nucleate pool boiling at four different pressures. International Journal of Heat and Mass Transfer, 2017, 112: 662–675
63. Gong M, Wu Y, Ding L, Cheng K, Wu J. Visualization study on nucleate pool boiling of ethane, isobutane and their binary mixtures. Experimental Thermal and Fluid Science, 2013, 51: 164–173
64. Yang Z, Gong M, Chen G, Zou X, Shen J. Two-phase flow patterns, heat transfer and pressure drop characteristics of R600a during flow boiling inside a horizontal tube. Applied Thermal Engineering, 2017, 120: 654–671
65. Zhuang X, Gong M, Chen G, Zou X, Shen J. Two-phase flow pattern map for R170 in a horizontal smooth tube. International Journal of Heat and Mass Transfer, 2016, 102: 1141–1149
66. Gong M, Song Q, Chen G, Zhuang X, Yang Z, Yao Y. Boiling heat transfer characteristics for methane, ethane and their binary mixtures. Heat Transfer Engineering, 2020, 41(1): 1–16
67. Song Q, Chen G, Xue H, Zhao Y, Gong M. R14 flow condensation heat transfer performance: measurements and modeling based on two-phase flow patterns. International Journal of Heat and Mass Transfer, 2019, 136: 298–311
68. Tang Q, Chen G, Yang Z, Shen J, Gong M Q. Numerical investigation on gas flow heat transfer and pressure drop in the shell side of spiral-wound heat exchangers. Science China. Technological Sciences, 2018, 61(4): 506–515
69. Zou X, Gong M, Wu J. A spiral tube heat exchanger with a variable diameter tube winding. China Patent, ZL 201510351126.8, 2017 (in Chinese)
70. Chen G, Gong M, Wu J. A plate-fin heat exchanger. China Patent, ZL 201510385761.8, 2017 (in Chinese)
71. Gong M, Wu J, Chen G. A reentrant flow plate-fin heat exchanger. China Patent, ZL 201310192611.6, 2015 (in Chinese)
72. Wu J, Gong M, Dong X, Shen J. A variable channel cross-sectional heat exchange. China Patent, ZL201210290661.3, 2015 (in Chinese)
73. Gong M, Wu J, Chen G, Dong X. A plate-fin heat exchanger with fluid flow back in the channel. China Patent, ZL201210553623.2, 2014 (in Chinese)
74. Li J, Gong M, Tang Q, Sun Z, Zou X, Chen G, Wu J. Design of coiled-wound heat exchanger in small plant of LNG. CIESC Journal, 2015, 66: 108–115 (in Chinese)
75. Song Q, Zhang J, Zhao Z, Luo J, Wang Q, Chen G. Development of natural gas liquefaction processes using mixed refrigerants: a review of featured process configurations and performance. Journal of Zhejiang University–Science A, 2019, 20(10): 727–780
76. Kountz K J, Kriha K, Liss W E, Perry M, Richards M, Zuckerman D. Development of a Small-Scale Natural Gas Liquefier. GTI Report for DOE, 2003
77. Nekså P, Brendeng E, Drescher M, Norberg B. Development and analysis of a natural gas reliquefaction plant for small gas carriers. Journal of Natural Gas Science and Engineering, 2010, 2(2–3): 143–149
78. Li K. Researches and practices of a small-scale liquefied natural gas apparatus. China Petroleum and Chemical Standard and Quality, 2012, 9: 100–101
79. Wang H. The research of the liquefaction technology in Shanxi Dingbian LNG plant. Refrigeration, 2013, 32(3): 23–29 (in Chinese)
80. Wang Q, Song Q, Zhang J, Liu R, Zhang S, Chen G. Performance analyses on four configurations of natural gas liquefaction process operating with mixed refrigerants and a rectifying column. Cryogenics, 2019, 97: 13–21
81. Liu Y M, Li D J. Natural gas liquefaction technology in Taian Shenran LNG plant. Cryogenics and Superconductivity, 2009, 11: 3–10